Contents lists available at iocspublisher

Science Midwifery

journal homepage: www.midwifery.iocspublisher.org

Review: Manufacturing Of Magnesium Oxide Nanoparticles As Antibacterial Agents

Citra Nurhashiva[1], Jessica Veronica[1], Lidia Intan Febriani[1], Risti Ragadhita[1], and Asep Bayu Dani Nandiyanto[1,*], Tedi Kurniawan[2]

[1]Departemen Pendidikan Kimia, Fakultas Pendidikan Matematika dan Ilmu Pengetahuan Alam, Universitas Pendidikan Indonesia, Jl. Dr. Setiabudi no. 229, Kota Bandung, 40154, Indonesia
[2]Engineering Technology Department, Community College of Qatar, Qatar

ARTICLE INFO

Keywords:
Nanoparticles,
Magnesium oxide,
Synthesis method

E-mail:
nandiyanto@upi.edu

ABSTRACT

The purpose of this article is to determine the most efficient method of synthesizing magnesium oxide nanoparticles as an antibacterial. The significant antibacterial activity of magnesium oxide was associated with the formation of Reactive Oxygen Species (ROS) on the surface of the oxide. In this article, the method of synthesizing magnesium oxide nanoparticles is discussed with the results of the study of the source material, method, advantages, and disadvantages of each method that can be used as a reference to choose which method is more efficient. Synthesis of magnesium oxides such as (1) synthesis of plant extracts, (2) combustion, (3) sonochemical synthesis, (4) sol-gel synthesis, and (5) solid-state. This synthesis method resulted in the characterization of magnesium oxide nanoparticles which were analyzed using X-ray Diffraction (XRD), Fourier Transform Infra-Red (FTIR), Field Emission Scanning Electron Microscopy (FESEM). The results showed that the most efficient method for synthesizing magnesium oxide as an antibacterial is the sol-gel synthesis method. The sol-gel method uses readily available materials, has a relatively low cost, easy procedure to perform, and was found to be a light and efficient route for large-scale industrial production of fine magnesium oxide nanoparticles as antibacterial.

1. Introduction

Nanostructured magnesium oxide has been widely used because of its unique properties, such as large band gap, thermodynamic stability, low dielectric constant, and low refractive index [1]. Magnesium is a cofactor in more than 300 enzyme systems that regulate various biochemical reactions in the body. Magnesium oxide, being a good source of magnesium, has thus become of biomedical importance [2]. MgO nanoparticles have become suitable candidates in the pharmaceutical industry as antibacterial and anticancer agents due to their high thermal and bioactive properties [3]**.** In biomedicine, magnesium oxide has been applied for bone repair, heartburn relief, and sensitive stomachs [4]. Recently, magnesium oxide nanoparticles have been used in cancer therapy in addition to having significant activity as an antibacterial agent [4],[5],[6],[7],[8]. This material becomes very interesting for many researchers to develop.

Magnesium oxide nanoparticles are highly ionic metal oxide nanoparticles with a very high surface area and unusual crystal morphology. Magnesium oxide nano has unique optical, electronic, magnetic, thermal, mechanical, and chemical properties due to its unique structure. Magnesium oxide is an important functional metal oxide that has been widely used in various fields, such as catalysis, refractory materials, paints, and superconductors [9]. To obtain the desired particle size, the size and morphology of the oxide particles can be modified using parameters such as pH, ionic strength, and different calcination temperatures. Usually, nanometer-sized particles (range 1-100 nanometers) are the main goal when synthesizing particles because nanoparticle-sized materials have unique properties compared to bulk materials [10].

The research literature used in this article has succeeded in producing magnesium oxide nanoparticles as antibacterials from various methods. This scientific article aims to determine the most efficient method of synthesizing magnesium oxide nanoparticles as an antibacterial. Several methods that can be used in the synthesis of magnesium oxide nanoparticles include combustion [10], synthesis of plant extracts [11], sonochemical synthesis [12], sol-gel synthesis [13], and solid-state synthesis [14]. Each method used in synthesizing magnesium oxide nanoparticles has its advantages, disadvantages, and different results, so a review is necessary. We must find the most

efficient method in the manufacture of magnesium oxide nanoparticles as antibacterial in terms of production costs (economic evaluation), safety, and impact on the environment. Currently, magnesium oxide nanoparticles have been used for the treatment of various ailments due to their biocompatible nature and remarkable stability under harsh conditions. In the field of medicine, magnesium oxide nanoparticles exhibit remarkable applications such as relief of heartburns, regeneration of bones, and as antitumor and antibacterial agents. Magnesium oxide nanoparticles showed potent antibacterial activity and antifungal activities against human pathogens The antibacterial efficacy of magnesium oxide nanoparticles might be due to their smaller sizes, which was consistent with the report that magnesium oxide nanoparticles with smaller sizes would exhibit potent bactericidal efficiency [7].

2. Method

Several methods are available for synthesizing magnesium oxide nanoparticles as an antibacterial, including combustion, the synthesis of plant extracts, sonochemical synthesis, sol-gel synthesis, and solid-state synthesis. Table 1. shows several methods of synthesizing magnesium oxide nanoparticles along with their result, advantages, and disadvantages.

TABLE 1.
MATERIALS, METHODS, RESULT, ADVANTAGE, DISADVANTAGE, AND REFERENCE

Material	Methods	Results	Advantages	Disadvantages	Reference
Magnesium Nitrate and Urea	Combustion	XRD study of magnesium oxide nanoparticles revealed the formation of a polycrystalline cubic structure of magnesium oxide nanoparticles. The average crystal size obtained is 27 nm	The technique is versatile, fast, and economical	Require high temperature	[10]
Manihot Esculenta Leaf and Magnesium Nitrate	Plant extract synthesis	The TEM assessment showed that the particles	Eco-friendly, safe, and cost-effective	Require a lot of tools to do the synthesis	[11]

Contents lists available at iocspublisher

Science Midwifery

journal homepage: www.midwifery.iocspublisher.org

Hexahydrate		were hexagonal and monodispersed with an average height uniformity of 36.7 nm.			
Magnesium Hydroxide, Natrium Hydroxide, and Bittern	Sonochemical Synthesis	Nanoparticles MgO with an average particle diameter of 195.7 nanometers.	The time required for the process is relatively fast	Use relatively expensive equipment	[12]
Arabic Gum	Sol-gel synthesis	IR spectrum of the sample calcined at 500°C for 4 hours showed a stretching vibration mode for the Mg-O-Mg section in the range of 587-681 cm^{-1} as a wide band. The wide band of vibrations is seen in the wavenumber range of 3325-3553 cm^{-1}	The materials used are natural, non-toxic, and stabilizer groups	Use expensive tools and materials, relatively long processing time, and large shrinkage during drying	[13]

Magnesium Acetate Tetrahydrate and Oxalic Acid Dihydrate	Solid-state synthesis	MgO nanoparticles with a large specific surface area of 213 $m^2 g^{-1}$. The MgO nanoparticles showed a robust adsorption capacity of 2375 mg g^{-1} towards Congo red.	Simple, low cost, low pollution.	Difficult control of reaction uniformity	[14]

2.1. Combustion Method

The solution combustion method is a versatile, fast, and economical technique for the synthesis of ceramic oxides. This method involves burning a redox mixture containing the stoichiometric ratio of the oxidizing agent and fuel in a preheated dampening furnace. Combustion is a fast and independent exothermic reaction between metal salts and organic fuels. A large amount of gas is generated during the combustion process to prevent the agglomeration of nanoparticles [10].

Magnesium nitrate is used as a precursor and urea as a fuel. Magnesium nitrate was dissolved in deionized water and urea as fuel was added to the precursor solution with constant stirring (1000 rpm). solution at ~70–80°C for 2 hours with continuous stirring. After the gel properties were formed, the dissolution was brought to room temperature, then transferred to a crucible which was placed in a muffle furnace at a temperature of 500°C for 3 hours. Due to heat energy, the combustion reaction occurs between the precursor (oxidizing agent) and urea (fuel). The white powder obtained is then ground using a mortar and pestle. The ground powder will be used for further analysis. In the combustion system, the desired product is prepared from a combustion reaction that takes place spontaneously at a high temperature at a high rate [10].

2.2. Synthesis Method Using Plant Extract

The green nanoparticle synthesis method is a synthesis method that forms metal nanoparticles with the help of natural materials derived from organisms (plants and microorganisms) both land and sea [11].

Preparation of extract from *Manihot esculenta* leaf water is by washing *Manihot esculenta* leaves using tap water and rinsing with deionized water to remove dust and particulate matter. Then, the leaves are dried and ground into a fine powder so that the surface becomes large for extraction. Extraction was carried out by boiling in a thermostatic water bath for 15 minutes. The extraction results were then added to a solution of $Mg(NO_3)_2.6H_2O$ in a beaker with constant stirring using a magnetic stirrer. The solid-liquid dispersion obtained was centrifuged. Then, the supernatant was removed and the residue was washed using deionized water to remove excess $Mg(NO_3)_2.6H_2O$ and residual organic molecules. Next, it was dried in an oven at 70°C for 2 hours and calcined in a furnace at 500°C for 3 hours to obtain magnesium oxide nanoparticles. The

Contents lists available at iocspublisher

Science Midwifery

journal homepage: www.midwifery.iocspublisher.org

obtained magnesium oxide nanoparticles were sonicated at 40°C for 1 hour in ultrasonic cleaning (CLEAN-120 HD) to disperse the particles [11].

2.3. Sonochemical Method

This research was conducted using bittern, sodium hydroxide, and 2-butanol. Bittern is a by-product of processing salt from seawater, while sodium hydroxide and 2-butanol used are PA (pro analysis) materials. Sample characterization was carried out using ICP - OES (Inductively Coupled Plasma - Optical Emission Spectrophotometers), XRD (X-Ray Diffraction), PSA (Particle Size Analyzer), and SEM-EDX (Scanning Electron Microscope-Energy Dispersive X-ray Disorders) Spectroscopy) [12].

First, the bittern is filtered to remove solid impurities. Magnesium hydroxide was synthesized by adding sodium hydroxide to sambiloto with a mole ratio of Mg^{2+} ion: sodium hydroxide = 1:2 according to the stoichiometric calculation then stirred at 300 rpm and a temperature of 30°C. The residue that has been separated from the filtrate is then dried in an oven for 24 hours at 100°C. The solid was calcined at 460°C for 2 h to produce magnesium oxide. Reduction of magnesium oxide particles from micro size to nano size is carried out by reference [12].

2 butanol is used as a sonication medium in the ultrasonic method. The amplitude was varied between 20%, 30%, and 40% while the sonication time was varied between 4, 8, and 16 minutes [12].

The concentration of magnesium and other impurities in the bittern and filtrate was analyzed using ICP-OES and calculated based on the mass balance to obtain the concentration of magnesium in the residue. XRD characterization was used to determine the phase composition of the residue before and after calcination. After the sonochemical process, the samples were analyzed using the free deposition method. Samples with the lowest supernatant height were analyzed using PSA and SEM-EDX to determine the size and morphology of the particles obtained [12].

2.4. Synthesis by Sol-Gel Method

Synthesis of magnesium oxide nanoparticles using gum arabic was carried out by dissolving gum arabic in distilled water and stirring for 120 minutes at 75°C to achieve a clean Arabic Gel (AG) solution. Then, $Mg(NO_3)_2.6H_2O$ was added to the AG solution and the container was placed in a sand bath. The temperature of the sand bath is 75°C and stirring is done for 14 hours to get a brown resin. The final product was calcined at 500°C in the air for 4 hours to obtain a white powder of magnesium oxide [13].

2.5. Solid-state Synthesis Method

In a typical synthesis of magnesium oxide nanoparticles, magnesium acetate tetrahydrate [$Mg(OAc)_2.4H_2O$, 10 mmol] is ground to a fine powder in an agate mortar and mixed with powdered oxalic acid dihydrate [$H_2C_2O_4.2H_2O$, 15 mmol] prepared by grinding in the other mortar. To ensure adequate contact of the reactants, the powder mixture obtained was ground to allow the chemical reaction to occur in the solid-state under ambient conditions through a wetting process until a dry white powder was obtained [14].

Some of the dry white powder obtained was sealed in a conical flask, then heated in a water bath at 60°C for 24 hours, then rinsed with distilled water several times, and dried at room temperature for 12 hours. Another part of the dry white powder obtained was directly calcined at temperatures of 450°C, 550°C, 650°C, and 750°C for 2 hours under air atmosphere to produce magnesium oxide nanoparticles with a heating rate of 2°C min- 1,5°C min^{-1}, and 10°C min^{-1} [14].

Oxalic acid dihydrate ($H_2C_2O_4.2H_2O$, 15 mmol) was replaced with NaOH (30 mmol). After rinsing and drying. The mixture obtained was calcined at 450°C for 2 hours under atmospheric air at a heating rate of 2°C min^{-1} to produce magnesium oxide nanoparticles [14].

3. Result and Analysis

The synthesized magnesium oxide nanoparticles showed promising and strong antibacterial and antifungal activity [15]. The explanation of the antibacterial effect of magnesium oxide nanoparticles from outside the cell lies in the chemical properties of magnesium oxide nanoparticles [16].

There are several suggested mechanisms, such as the liberation of reactive oxygen species (ROS), interaction of magnesium oxide nanoparticles with microbial cells, after which they destroy pathogens, and the influence of bases are proposed to describe the antimicrobial action mechanism of magnesium oxide nanoparticles. Several studies have reported that the antimicrobial mechanism of magnesium oxide nanoparticles is due to the development of ROS Like superoxide anion (O_2) [17].

It is known that the considerable antibacterial activity of magnesium oxide is associated with the formation of Reactive Oxygen Species (ROS) on the surface of the oxide. Magnesium oxide nanoparticles have a large number of oxygen vacancies on their surface which are adsorbed on the bacterial cell wall. The formation of superoxide radicals on the surface of microorganisms indicates the presence of oxygen vacancies on the cell surface. Superoxide radicals are highly reactive species that induce their effects by disrupting the carbonyl groups of peptide bonds in cell walls and membranes. Superoxide radicals induced by magnesium oxide nanoparticles can cause damage to cell membrane integrity resulting in leakage of intracellular material followed by cell death [16].

3.1. Combustion Method

The structure of the sample was analyzed by X-ray diffractometer (XRD) using CuKα (1.5418Å) radiation. The sample is scanned in the range of 20-90° with a step size of 0.02°. FTIR spectrometer was used to confirm the presence of bonds in the wavenumber range of 400-4000 cm^{-1} with a resolution of 0.5 cm^{-1}. The absorbance values of the samples were analyzed using a UV–Visible dual-beam spectrophotometer with a resolution of 1 nm. Surface morphology and composition were observed using a field emission scanning electron microscope (FESEM) [10].

- X-Ray Diffraction Studies (XRD)

XRD analysis was carried out in the range of 20-80° (2θ) using CuKα radiation. XRD study of magnesium oxide nanoparticles showed peaks at angles of 18.57°, 36.96°, 38.02°, 42.98°, 62.36°, 74.71°, and 78.66° corresponding to (1 1 1), (0 0 2), (2 0 2), (1 1 3), and (2 2 2) which reveal the formation of a polycrystalline cubic structure from magnesium oxide nanoparticles. No other impurity phases were found in the XRD pattern. Figure 1. shows the XRD pattern shows high-intensity orientation peaks (0 0 2) indicating high crystallinity of the synthesized material. The average crystal size was calculated using reflection (0 0 2) and obtained 27 nm [10].

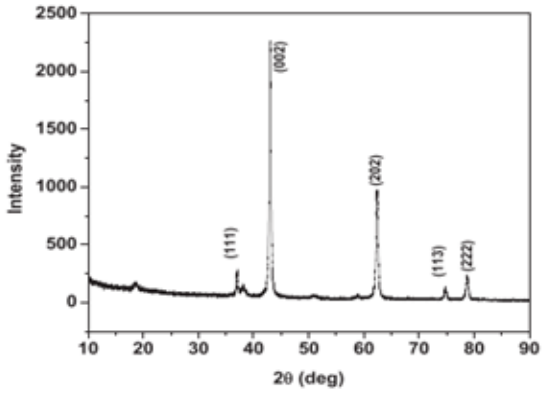

Figure 1. XRD pattern of magnesium oxide nanoparticles.

- FTIR Spectroscopy

The FTIR spectrum of magnesium oxide nanoparticles prepared using the combustion process showed a strain vibrational mode of ~0600-850 cm^{-1}. This strain vibration mode indicates the

Contents lists available at iocspublisher

Science Midwifery

journal homepage: www.midwifery.iocspublisher.org

presence of Mg-O-Mg bonds. A different band was observed at the wavenumber ~1434 cm^{-1} indicating the flexural vibration of the surface hydroxyl groups. A wideband was observed to be ~3268 cm^{-1} due to the O–H stretching vibrations of the water molecules. The peak width in the range of 3300-3600 cm^{-1} indicates the formation of magnesium oxide nanoparticles [10].

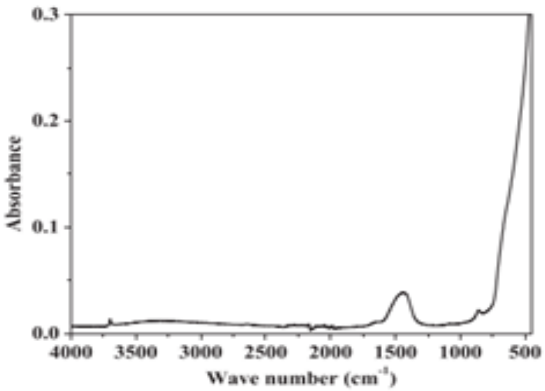

Figure 2. FTIR spectrum of magnesium oxide nanoparticles.

- Field emission scanning electron microscopy study

Figure 2 shows the surface topography of magnesium oxide nanoparticles. Figures 3 and 4 show the formation of crystals with different magnifications (200 and 100 k magnification) [10].

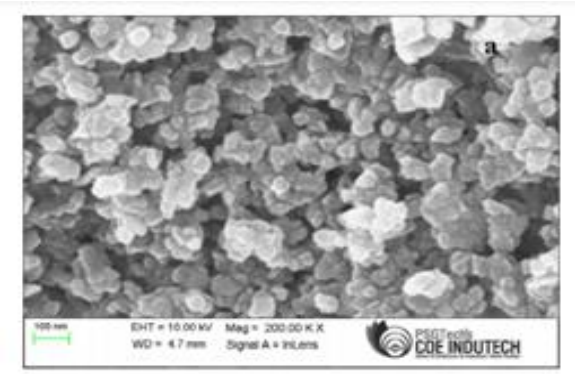

Figure 3. FESEM images of the magnesium oxide nanoparticles with 200 k magnifications.

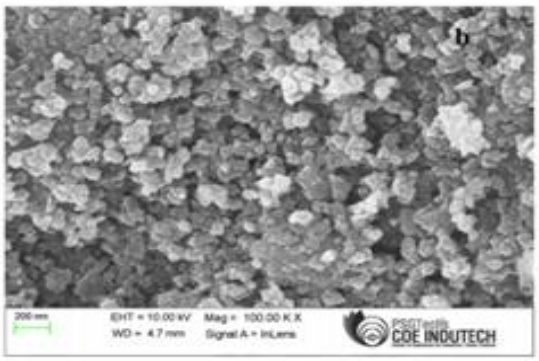

Figure 4. FESEM images of the magnesium oxide nanoparticles with 100 k magnifications.

3.2. Synthesis Method Using Plant Extract

Morphological studies to assess the microstructure, particle distribution, and composition of magnesium oxide nanoparticles were carried out in a scanning electron microscope (SEM) equipped with an X-ray analyzer (EDX) energy dispersion unit (SEM: JEOL JSM 7660F). The samples were analyzed at an accelerating voltage of 15 kV. It is known that there are Mg atoms and O atoms in the sample at high intensity. The atomic ratio is 1:1 as in pure magnesium oxide compounds. The carbon atoms observed in the spectrum are derived from various organic biomolecules in plant extracts that act as reducing groups and capping groups during the reaction for the formation of magnesium oxide nanoparticles [11].

The particle size and structure of magnesium oxide nanoparticles were determined using a transmission electron microscope (TEM: JEM-ARM200F-G) with an accelerating voltage of 200 kV. Then, the average particle size was determined from SEM and TEM micrographs using ImageJ software. The morphology of magnesium nanoparticles is presented in Figure 5. The microstructure shows hexagonal particles of average size 37.3 nm appearing as different ensembles. The particles showed a very little degree of agglomeration and were well distributed over the surface of the material to present a large surface area-to-volume ratio. The TEM assessment showed that the particles were hexagonal and monodispersed with an average high size uniformity of 36.7 nm. The hexagonal properties of the particles were first discovered using SEM micrographs and on TEM micrographs showed crystalline properties. Mean particle size measurements of magnesium oxide nanoparticles from SEM micrographs (37.30 nm) were compared with results from TEM micrographs (36.90 nm) using ImageJ and demonstrated dimensional validation of magnesium oxide nanoparticles [11].

Figure 6. shows the presence of Mg and O in the sample at high intensity and at a 1:1 atomic ratio as found in pure MgO compound. The carbon atom observed in the spectrum is from the various organic biomolecules present in the plant extract which acted as reducing and capping agents during the reaction to form the magnesium oxide nanoparticle [11].

The diffraction pattern of magnesium oxide nanoparticles was evaluated in an X-ray diffractometer (XRD: Rigaku D/Max IIIC) to observe the type of phase in the sample, the crystal structure of the magnesium oxide nanoparticles, and the purity of the sample phase. It was found that the diffraction pattern showed various peaks corresponding to the reflection field. No other peaks were observed indicating the absence of metallic impurities and this supports the EDX results. As observed in the diffractograms shown in Figure 7, the diffraction pattern shows various peaks corresponding to (111), (200), (220), (311), and (222) refection planes [11].

Fourier transform infrared spectroscopy (FTIR: Nicolet iS10) with a wave number of 350-4000 cm^{-1} was used to analyze the type of bond in magnesium oxide nanoparticles. This is to complement and confirm the results of the analysis with GC-MS, UV, and XRD. The FTIR spectrum of magnesium oxide nanoparticles shows a broad absorption band centered on 3421 cm^{-1} due to the stretching vibration of the O-H group in the alcohol resulting from the reaction of the phytochemical hydroxyl limiting group in the leaf extract with magnesium oxide particles. Other peaks were also found indicating the presence of C-H, N-H, Mg-O, C-O, C-O-C groups, and hexagonal magnesium oxide nanoparticles. The FTIR spectrum of the magnesium nanoparticles is depicted in Figure 8. Figure 8 shows a broad absorption band centered at 3421 cm−1 due to the stretching vibration of the O–H group in alcohol, which results from the capping reaction of the hydroxyl group of the phytochemicals in the leaf extract with the MgO particle [11].

Based on the experimental results in the synthesis using the aqueous extract of *Manihot esculenta* leaves, several organic biomolecules were found as reducing agents and limiting agents to form magnesium oxide nanoparticles when identified using GC-MS. Analysis performed using UV-Vis spectrophotometry, SEM/EDX, TEM, XRD, and FTIR confirmed that magnesium oxide nanoparticles are hexagonal with an average diameter of 35.7 nm. Based on the protocol defined in this study, it is possible to obtain monodispersed magnesium oxide nanoparticles of uniform shape and size [11].

Contents lists available at iocspublisher

Science Midwifery

journal homepage: www.midwifery.iocspublisher.org

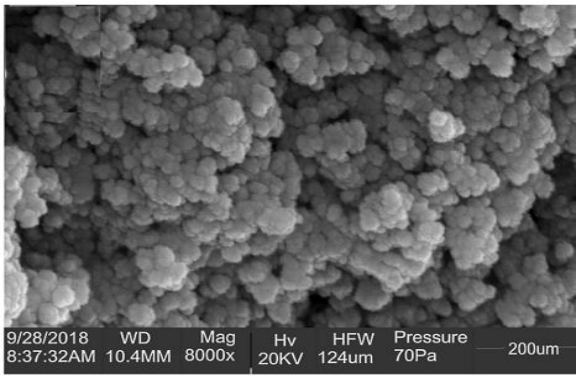

Figure 5. SEM micrograph of magnesium oxide nanoparticles shows well-distributed particles.

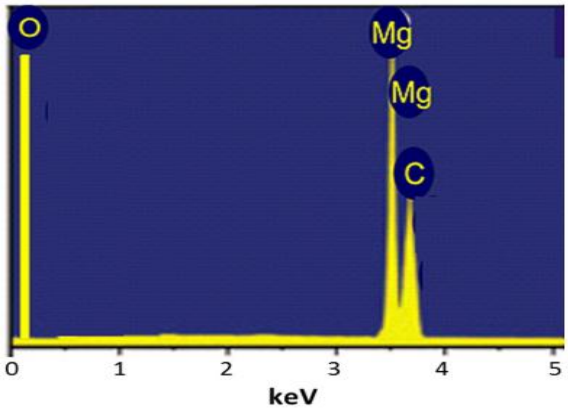

Figure 6. The EDX spectrum of the magnesium oxide nanoparticles showed the presence of Mg atoms and O atoms at a 1:1. atomic ratio.

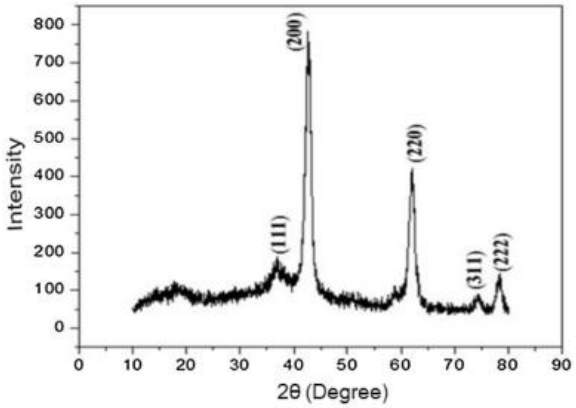

Figure 7. XRD pattern of magnesium oxide nanoparticles shows monophasic magnesium oxide.

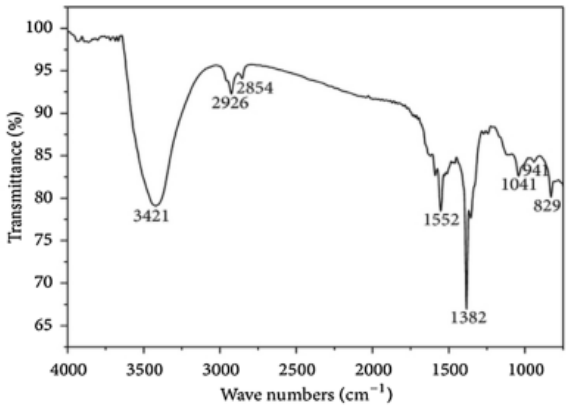

Figure 8. The FTIR spectra of the synthesized magnesium oxide nanoparticles showed the bonding associated with the capping biomolecules contained in the *M. esculenta* leaf extract method and magnesium oxide.

3.3. Sonochemical Method

The XRD diffractogram of the residue obtained from the reaction between bittern and sodium hydroxide is shown in Figure 9. From Figure 9., it can be seen that the position of the main crystal peak is magnesium hydroxide. This peak is followed by several small peaks of sodium chloride [12].

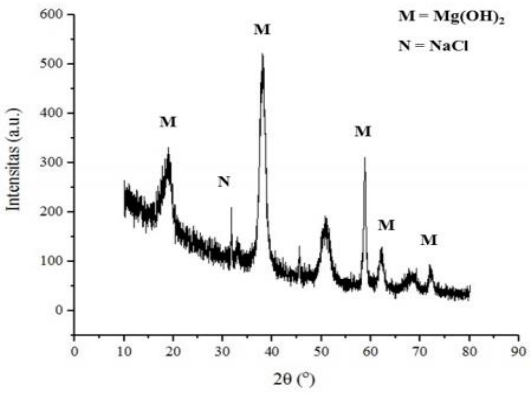

Figure 9. XRD diffractogram of magnesium hydroxide.

Magnesium hydroxide is calcined at 460°C for 2 hours to produce magnesium oxide. The XRD diffractogram of the calcined results can be seen in Figure 10. The absence of magnesium hydroxide peaks indicates that magnesium hydroxide has completely decomposed in the calcination process to produce magnesium oxide. This magnesium oxide peak is also followed by several minor sodium chloride peaks [12].

Contents lists available at iocspublisher

Science Midwifery

journal homepage: www.midwifery.iocspublisher.org

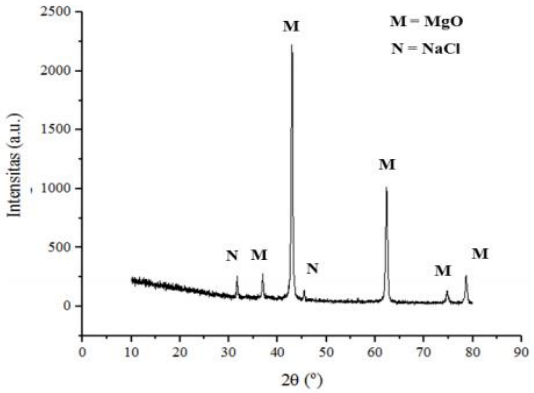

Figure 10. XRD diffractogram of magnesium oxide.

In Figure 11., the morphology of the sample can be observed through SEM analysis at 5000x magnification. The particles in this image have a spherical shape, similar to previous studies [12].

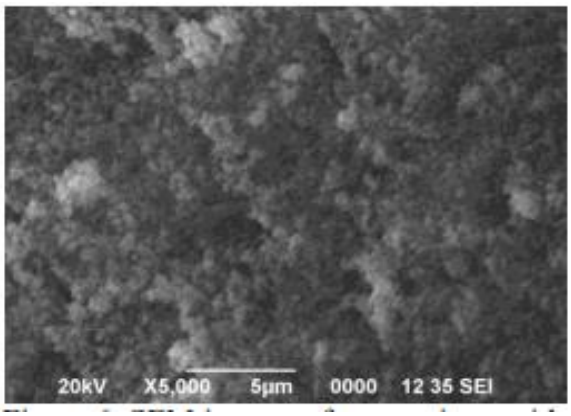

Figure 11. SEM images of magnesium oxid**e**.

3.4. Sol-Gel Method

In the experimental results of the synthesis using the sol-gel method using gum arabic, it was found in Figure 12. that the IR spectrum of the sample calcined at 500°C for 4 hours showed a stretching vibration mode for the Mg-O-Mg section in the range of 587-681 cm^{-1} as a wide band. The wide band of vibrations is seen in the wavenumber range of 3325-3553 cm^{-1} due to the O-H stretching vibration of the adsorbed water molecules and surface hydroxyl groups. This is due to the air adsorption of water molecules onto the magnesium oxide surface when exposed to the atmosphere. Figure 13. shows The room temperature UV-Vis absorption spectrum of the MgO. The green synthesis of magnesium oxide nanoparticles shows an absorbance spectrum at 200 nm in UV-Vis spectroscopy which is associated with the formation of magnesium oxide nanoparticles. Crystal structure confirmation analysis was performed using X-ray diffraction (XRD) patterns. Figure 14. shows the XRD pattern of the product was obtained by calcining the precursor at 500°C. In XRD analysis, a series of peaks at 2θ can be assigned to each field. The resulting diffraction peaks are strong and sharp, confirming the high crystallinity of the product. The Scherrer formula is the average crystal size of magnesium oxide nanoparticles determined from the full width at half maximum (FWHM) of the XRD pattern and the average size of magnesium oxide nanoparticles is 14 nm. The Williamson Hall equation was used to calculate the crystal size as well as the sample microstrain. The microstrain is calculated from the slope of the straight line that fits the W-H plot.

The negative slope represents the compressive strain, while the positive slope is the tensile strain. It was found that the compressive strain was in the annealed sample [13].

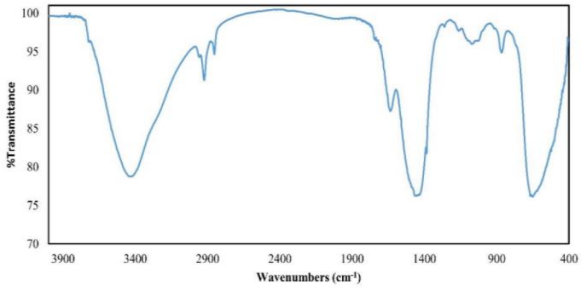

Figure 12. FT-IR spectrum of magnesium oxide nanoparticles.

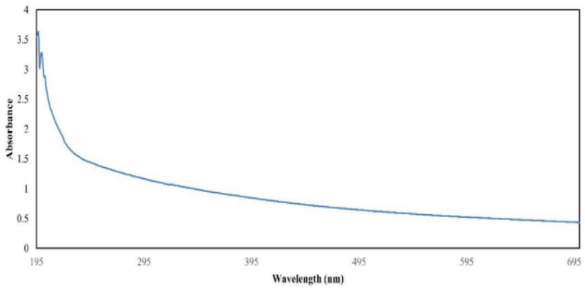

Figure 13. UV-Vis spectrum of magnesium oxide nanoparticles.

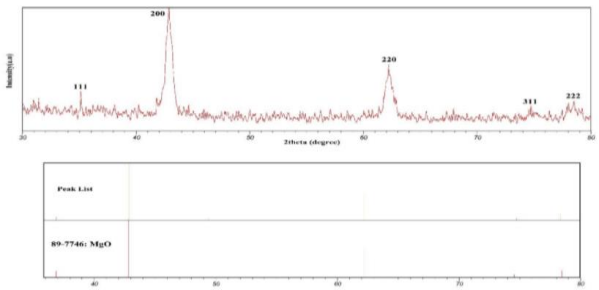

Figure 14. XRD pattern of synthesized magnesium oxide nanoparticles.

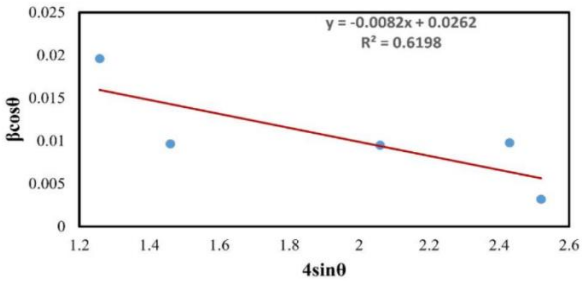

Figure 15. Williamson Hall Plot for magnesium oxide nanoparticles.

Contents lists available at iocspublisher

Science Midwifery

journal homepage: www.midwifery.iocspublisher.org

The Williamson Hall equation was used to calculate the crystallite size as well as the Micro strain of the sample, which equation was shown below:

$$\beta\cos\theta = K\lambda/D + 4\varepsilon\sin\theta \quad (1)$$

3.5. Solid-State Synthesis Method

In the last experiment, the solid-state method, it was explained that magnesium oxide nanoparticles showed a strong adsorption capacity of 2375 mg g^{-1} against Congo red. Raw materials and calcination temperature affect particle size, specific surface area, and surface alkalinity which in turn affect the adsorption properties. The outstanding adsorption capacity is attributed to the hydrogen bonding between the hydrogen atom of the –OH group on the surface of the magnesium oxide and the nitrogen or oxygen atom of the characteristic functional group in Congo red, as well as the electrostatic interaction between the surface of the positively charged magnesium oxide and the anionic Congo red dye [14].

Figure 16a. shows the synthesis of MgO nanoparticles was achieved through the simple solid-state chemical reaction between magnesium acetate and oxalic acid. The typical SEM image in Figure 16b shows the resulting MgO, in which the uniform particles were directly observed. Figure 16c shows TEM and HRTEM images of the MgO nanoparticles with average particle diameters of approximately 10 nm, indicating a distinct lattice space of 0.21 nm. The crystal phase of the as-obtained product was analyzed by XRD, as shown in Figure 16d. All XRD diffraction peaks of the as-prepared samples were in good agreement with the diffraction peaks of the main characteristic planes, (200), (220), and (222), of MgO (JCPDS card no. 74-1225). Figure 16e shows the N_2 adsorption-desorption isotherm and corresponding pore size distribution curve (inset) of the as-synthesized MgO products exhibited a typical type-IV isotherm with a significant H3 hysteresis loop, which are typical characteristics of a porous structure [14].

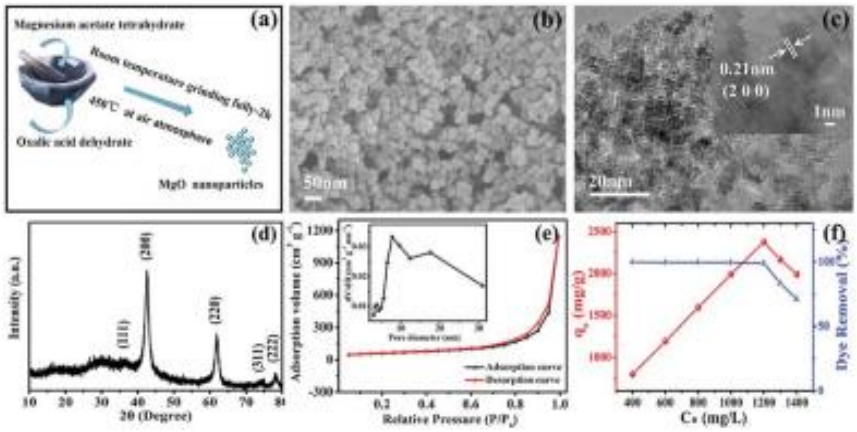

Figure 15. (a) Fabrication scheme, (b) SEM image, (c) TEM and HR-TEM (inset) images, (d) XRD pattern, (e) N_2 adsorption-desorption isotherms and pore size distribution curves (inset), and (f) adsorption isotherm of congo red on the magnesium oxide nanoparticles.

4. Conclusion

In the manufacture of magnesium oxide nanoparticles, several methods can be used to synthesize magnesium oxide, namely the synthesis of plant extracts, combustion, sonochemical synthesis, sol-gel synthesis, and solid-state. Of these several methods, the most efficient method for synthesizing magnesium oxide is the sol-gel synthesis method. This is because the sol-gel method uses materials that are easy to obtain, have relatively low prices, have easy procedures to carry out, and is a lightweight and efficient route for large-scale industrial production of fine magnesium

oxide nanoparticles as antibacterial. The significant antibacterial activity of magnesium oxide was associated with the formation of Reactive Oxygen Species (ROS) on the surface of the oxide.

Acknowledgments

We acknowledged Bangdos, Universitas Pendidikan Indonesia.

References

[1] R. Prasanth, S. Kumar, A. Jayalakshmi, and G. Singaravelu, "Green synthesis of magnesium oxide nanoparticles and their antibacterial activity," *Indian J. Geo Mar. Sci.*, vol. 48, no. 08, pp. 1210–1215, 2019, [Online]. Available: http://nopr.niscair.res.in/handle/123456789/49711.

[2] P. Bhattacharya, S. Swain, L. Giri, and S. Neogi, "Fabrication of magnesium oxide nanoparticles by solvent alteration and their bactericidal applications," *J. Mater. Chem. B*, vol. 7, no. 26, pp. 4141–4152, 2019, [Online]. Available: https://pubs.rsc.org/en/content/articlehtml/2019/tb/c9tb00782b.

[3] J. Jeevanandam, Y. S. Chan, and M. K. Danquah, "Calcination-Dependent Morphology Transformation of Sol-Gel-Synthesized MgO Nanoparticles," *ChemistrySelect*, vol. 2, no. 32, pp. 10393–10404, Nov. 2017, doi: 10.1002/SLCT.201701911.

[4] C. W. Wong *et al.*, "Response Surface Methodology Optimization of Mono-dispersed MgO Nanoparticles Fabricated by Ultrasonic-Assisted Sol–Gel Method for Outstanding Antimicrobial and Antibiofilm Activities," *J. Clust. Sci.*, vol. 31, no. 2, pp. 367–389, Mar. 2020, doi: 10.1007/S10876-019-01651-3.

[5] K. Karthik, S. Dhanuskodi, C. Gobinath, S. Prabukumar, and S. Sivaramakrishnan, "Fabrication of MgO nanostructures and its efficient photocatalytic, antibacterial and anticancer performance," *J. Photochem. Photobiol. B Biol.*, vol. 190, pp. 8–20, 2019, [Online]. Available: https://www.sciencedirect.com/science/article/pii/S1011134418306997.

[6] K. Karthik, S. Dhanuskodi, C. Gobinath, S. Prabukumar, and S. Sivaramakrishnan, "Ultrasonic-assisted CdO–MgO nanocomposite for multifunctional applications," *Taylor Fr.*, vol. 34, no. 7, pp. 403–414, Jun. 2019, doi: 10.1080/10667857.2019.1574963.

[7] A. Pugazhendhi, R. Prabhu, K. Muruganantham, R. Shanmuganathan, and S. Natarajan, "Anticancer, antimicrobial and photocatalytic activities of green synthesized magnesium oxide nanoparticles (MgONPs) using aqueous extract of Sargassum wightii," *Elsevier*, vol. 190, pp. 86–97, 2019, [Online]. Available: https://www.sciencedirect.com/science/article/pii/S1011134418312090.

[8] K. Karthik, S. Dhanuskodi, S. P. Kumar, C. Gobinath, and S. Sivaramakrishnan, "Microwave assisted green synthesis of MgO nanorods and their antibacterial and anti-breast cancer activities," *Elsevier*, vol. 206, pp. 217–220, 2017, [Online]. Available: https://www.sciencedirect.com/science/article/pii/S0167577X17310418.

[9] R. Dobrucka, "Synthesis of MgO Nanoparticles Using Artemisia abrotanum Herba Extract and Their Antioxidant and Photocatalytic Properties," *Iran. J. Sci. Technol. Trans. A Sci.*, vol. 42, no. 2, pp. 547–555, Jun. 2018, doi: 10.1007/S40995-016-0076-X.

[10] G. Balakrishnan, R. Velavan, K. M. Batoo, and E. H. Raslan, "Microstructure, optical and photocatalytic properties of MgO nanoparticles," *Elsevier*, vol. 16, p. 103013, 2020, [Online]. Available: https://www.sciencedirect.com/science/article/pii/S221137971933493X.

[11] E. R. Essien, V. N. Atasie, A. O. Okeafor, and D. O. Nwude, "Biogenic synthesis of magnesium oxide nanoparticles using Manihot esculenta (Crantz) leaf extract," *Int. Nano Lett.*, vol. 10, no. 1, pp. 43–48, Mar. 2020, doi: 10.1007/S40089-019-00290-W.

[12] F. E. Yunita, N. C. Natasha, E. Sulistiyono, A. R. Rhamdani, A. Hadinata, and E. Yustanti, "Time and Amplitude Effect on Nano Magnesium Oxide Synthesis from Bittern using Sonochemical Process," *IOP Conf. Ser. Mater. Sci. Eng.*, vol. 858, p. 012045, 2020, doi: 10.1088/1757-899X/858/1/012045.

[13] S. Taghavi Fardood, A. Ramazani, and S. Woo Joo, "Eco-friendly synthesis of magnesium oxide nanoparticles using arabic Gum," *J. Appl. Chem. Res.*, vol. 12, pp. 8–15, 2018, [Online]. Available: http://jacr.kiau.ac.ir/article_536684_f173fdf64b46d4f6ef6c4f729e72681c.pdf.

[14] H. Zhang, J. Hu, J. Xie, S. Wang, and Y. Cao, "A solid-state chemical method for synthesizing MgO nanoparticles with superior adsorption properties," *RSC Adv.*, vol. 9, pp. 2011–2017, 2019, [Online]. Available: https://pubs.rsc.org/en/content/articlehtml/2019/ra/c8ra09199d.

[15] G. S. El-Sayyad, F. M. Mossalam, and A. I. El-Batal, "One-pot green synthesis of magnesium oxide nanoparticles using Penicillium chrysogenum melanin pigment and gamma rays with antimicrobial activity against," *Elsevier*, vol. 29, no. 11, pp. 2616–2625, 2018, [Online]. Available: https://www.sciencedirect.com/science/article/pii/S0921883118303169.

[16] J. Maji, S. Pandey, S. B.-B. of M. Science, and U. 2020, "Synthesis and evaluation of antibacterial properties of magnesium oxide nanoparticles," *Springer*, vol. 43, no. 1, pp. 1–10, Dec. 2020, doi: 10.1007/s12034-019-1963-5.

[17] A. Baraka, S. Dickson, M. Gobara, G. E.-S.-C. Papers, and undefined 2017, "Synthesis of silver nanoparticles using natural pigments extracted from Alfalfa leaves and its use for antimicrobial activity," *Springer*, vol. 71, no. 11, pp. 2271–2281, Nov. 2017, doi: 10.1007/s11696-017-0221-9.